

Chapter 6

Fundamental Physics with Antihydrogen

J. S. Hangst

Abstract Antihydrogen—the antimatter equivalent of the hydrogen atom—is of fundamental interest as a test bed for universal symmetries—such as CPT and the Weak Equivalence Principle for gravitation. Invariance under CPT requires that hydrogen and antihydrogen have the same spectrum. Antimatter is of course intriguing because of the observed baryon asymmetry in the universe—currently unexplained by the Standard Model. At the CERN Antiproton Decelerator (AD) [1], several groups have been working diligently since 1999 to produce, trap, and study the structure and behaviour of the antihydrogen atom. One of the main thrusts of the AD experimental program is to apply precision techniques from atomic physics to the study of antimatter. Such experiments complement the high-energy searches for physics beyond the Standard Model. Antihydrogen is the only atom of antimatter to be produced in the laboratory. This is not so unfortunate, as its matter equivalent, hydrogen, is one of the most well-understood and accurately measured systems in all of physics. It is thus very compelling to undertake experimental examinations of the structure of antihydrogen. As experimental spectroscopy of antihydrogen has yet to begin in earnest, I will give here a brief introduction to some of the ion and atom trap developments necessary for synthesizing and trapping antihydrogen, so that it can be studied.

6.1 Some History

Antihydrogen was initially produced and observed in in-beam experiments at CERN and Fermilab [2, 3], but these experiments had little potential for future measurements of the antihydrogen spectrum, and were quickly abandoned. During the operation

J. S. Hangst (✉)

Department of Physics and Astronomy, Aarhus University, DK-8000 Aarhus C Denmark
and CERN Division PH, CH-1211 Geneve 23, Switzerland
e-mail: jeffrey.hangst@cern.ch

of the LEAR facility at CERN, the TRAP collaboration developed the necessary techniques for slowing, cooling, and trapping antiprotons [4, 5]. In parallel, Surko and colleagues developed the technology for accumulating and storing positrons [6] emitted from a radioactive source. The Surko technique was adapted for antihydrogen production by the ATHENA collaboration [7] at the AD. ATHENA successfully demonstrated synthesis of antihydrogen atoms from trapped plasmas of antiprotons and positrons in 2002 [8]. Following the 1-year shutdown of the AD in 2005, the ATRAP and ALPHA (successor to ATHENA) collaborations embarked on efforts to magnetically trap neutral antihydrogen atoms. The ALPHA collaboration succeeded in trapping atoms of antihydrogen in 2010 [9]. Progress with trapped antihydrogen has been brisk in recent years. ALPHA has shown that it is possible to hold trapped anti-atoms for up to 1,000 s [10], and to drive resonant quantum microwave transitions (positron spin flip) in the trapped atoms [11]. More recently, ALPHA has performed the first systematic study of antihydrogen atoms in gravitational free fall [12]. ATRAP has reported evidence for trapped antihydrogen atoms [13], although the experiment appears to suffer from a lack of reproducible conditions. Using a very different approach, the ASACUSA collaboration hopes to study the hyperfine spectrum of antihydrogen atoms in flight [14]. They have recently demonstrated progress on generating a beam of antihydrogen atoms produced in their novel cusp trap [15]. Two new experiments at the AD hope to study the effect of the Earth's gravitational field on antihydrogen atoms. The AEgIS experiment [16] began operation in 2012, and the Gbar experiment [17] should begin in a few years. It is fair to say that there has never been more activity in low-energy antihydrogen physics than at the present time. In the following I will concentrate on the experimental techniques that have been developed to produce trappable antihydrogen atoms. The point of reference will of course be the authors ALPHA and ATHENA experiments, but differences between these approaches and those of other groups will be noted along the way. This chapter is intended as an overview, with the technical details to be found in the referenced literature.

6.2 Producing Antihydrogen: ATHENA

The basic idea for producing antihydrogen atoms is deceptively simple. Clouds of positrons and antiprotons, stored in Penning traps, are mixed, i.e., allowed to spatially overlap and interact (we will not review all of the techniques for catching and accumulating antiprotons and positrons here; see the above-referenced literature). The basic workhorse potential used for mixing is the so-called nested potential [18], shown in Fig. 6.1. The positrons are trapped in the center well of the nested potential. In the ATHENA solenoidal field of 3 T, the positrons would cool by cyclotron radiation and attempt to come into equilibrium with the surrounding trap structure—which was at about 15 K; however, no absolute measure of temperature was available in ATHENA. The antiprotons were injected from a side well (Fig. 6.1) and would interact in the positron cloud to form antihydrogen. The dominant formation mechanism

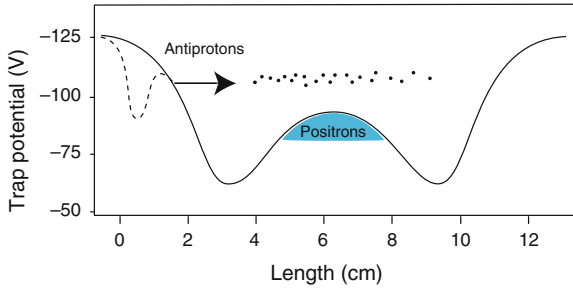


Fig. 6.1 The potential well configuration used in the first demonstration of low energy antihydrogen production by ATHENA. Antiprotons were injected from the well at the left of the figure (*dashed line*) into the nested potential well (reproduced from [8])

is a three-body event involving two positrons and an antiproton—the extra positron carries away the binding energy of the atom. Three-body formation typically results in loosely-bound Rydberg atoms. In ATHENA, a typical mixing cycle involved a few tens of thousands of antiprotons and up to 10^8 positrons. Several thousand antihydrogen atoms could be produced per cycle, with a peak rate of a few hundred per second [19].

6.3 Detecting Antihydrogen: ATHENA

The charged particles used to make antihydrogen are confined by the fields of the Penning trap. When a neutral antihydrogen atom forms, it is insensitive to the trapping fields and escapes, to annihilate on the inner surface of the trap electrodes. ATHENA pioneered the method of annihilation detection to identify the lost atoms when they hit the wall [7]. The ATHENA detector is shown schematically in Fig. 6.2. The two-layer silicon detector could identify the tracks of charged pions from the antiproton annihilation, and the CsI crystals detected the back-to-back, 511 keV gamma rays from positron annihilation. Spatial and temporal coincidence of these two signatures on the wall of the Penning trap provided the first confirmation for production of low energy antihydrogen [7]. Spatial characterization of the antihydrogen annihilation distribution proved to be a powerful tool for studying and optimising antihydrogen production in ATHENA [20]. For example, it is possible to distinguish antihydrogen annihilation from the annihilation of bare antiprotons lost from the trap (or resulting from field ionisation of anti-atoms) without relying on the positron detection. A position sensitive annihilation detector is also a key feature of the ALPHA antihydrogen trapping apparatus; see below. Note that the ATRAP collaboration has relied heavily on field-ionisation detection of Rydberg antihydrogen for their production experiments [21]. In this technique, a drifting Rydberg anti-atom

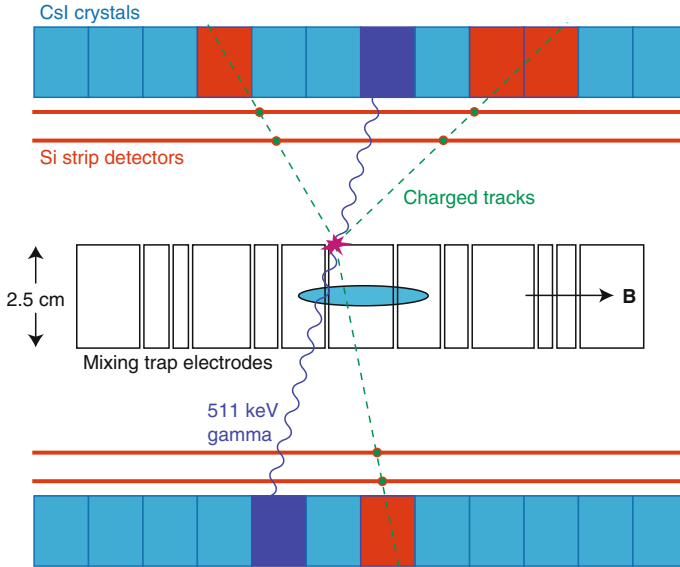


Fig. 6.2 Schematic diagram of the ATHENA antihydrogen production trap and annihilation detector. The *dashed green lines* represent charged pion tracks from an antiproton annihilation; the *wavy blue lines* are 511 keV gammas from a positron annihilation. The location of the positron plasma is indicated by the *blue shape* at the center of the Penning trap, which employed a 3 T axial field (reproduced from [8])

is stripped by a spatially localized electric field, and the freed antiproton is re-trapped, to be released, detected and counted at a later time. This technique cannot be applied to antihydrogen in the ground state—which is the ultimate system of interest.

6.4 Antihydrogen and Ion Trap Physics

Production of antihydrogen requires careful control and manipulation of one component plasmas of electrons, antiprotons and positrons. The Penning traps employed comprise solenoidal magnetic fields of typically a few T, and stacks of hollow, cylindrical electrodes that can be used to create and dynamically manipulate longitudinal electric fields. (see Figs. 6.1 and 6.2.) The traps are typically placed in contact with a liquid helium cryostat for thermal and vacuum considerations. Electrons are used to cool the trapped antiprotons—which have initial energies of up to several keV—down to cryogenic temperatures [5]. Electrons pre-loaded into the catching well cool through cyclotron radiation in the solenoidal magnetic field. A bunch of antiprotons from the AD (5.3 MeV kinetic) can be dynamically trapped using a pulsed, high voltage electrode. The antiprotons are either slowed by passing through a thin foil (ATRAP, ATHENA, ALPHA) or are first decelerated to 100 keV by a radiofrequency

quadrupole before the final degrading stage (ASACUSA). The AD cycle is typically about 100s in duration and results in about 3×10^7 antiprotons delivered to the experiment in each cycle.

Many complex manipulations of the plasmas are necessary to produce antihydrogen reproducibly. The electrons must first be removed from the combined electron-antiproton plasma before antihydrogen formation can proceed. In ALPHA, this plasma would typically comprise several tens of millions of electrons and about 50,000 antiprotons. The electrons are removed by pulsing open the confining potential for intervals short enough that the faster electrons can escape while the antiprotons remain trapped. This process inevitably heats the antiprotons—so even if the initial mixed plasma was close to the cryogenic wall temperature, the antiprotons will typically end up at a few hundred K. We will consider further cooling of antiprotons later.

Luckily, just producing antihydrogen doesn't require terribly cold antiprotons. The antiprotons are typically injected into a much colder positron plasma and can be cooled by Coulomb collisions inside the positron cloud. Indeed, in the initial ATHENA experiments, antiprotons were injected into the positron plasma with tens of eV of longitudinal energy (note that 1 eV is equivalent to about 12,000 K). Temperature plays a much more important role when we discuss trapping of antihydrogen later.

Plasma radii and densities must also be controlled. The rotating wall technique [22] plays a crucial role in production of antihydrogen cold enough to trap, and is also typically used for tailoring electron and positron densities in any production experiment. In ALPHA, the rotating wall compression technique is used extensively: on electrons, on positrons, and on combined electron/antiproton plasmas [23]. It is obviously important to have reliable diagnostics for measuring the transverse sizes and density distributions of the trapped plasmas. In ALPHA we have relied heavily on microchannelplate/phosphor screen detectors [24]. The trapped cloud is extracted longitudinally from the trap and dumped onto the imaging detector. A rather extreme example of an unstable antiproton cloud extracted from the ALPHA-2 device is shown in Fig. 6.3. Note that linear tracks from the annihilation products can be seen traversing the face of the detector. ASACUSA has used similar detectors to study rotating wall compression of plasmas in their traps [25]. Monitoring of plasma vibrational modes has also proved to be a useful technique for diagnosing the behaviour of lepton plasmas for antihydrogen production and related experiments. In particular, monitoring changes in temperature through changes in the quadrupole frequency [26, 27] was very useful in ATHENA [28, 29]. In ALPHA we have recently used similar electron plasma mode diagnostics to study the effect of injected microwaves, resonant at the cyclotron frequency, on stored electrons, and used this information to help characterize the microwave field profile [30] for the antihydrogen spin flip experiment [11].

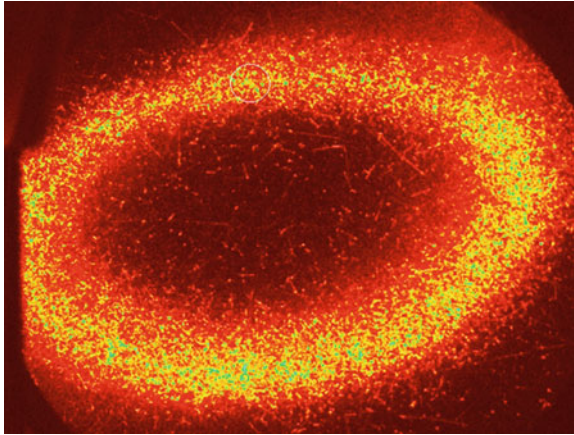


Fig. 6.3 A false color image of an antiproton plasma extracted from the ALPHA-2 device. The antiprotons strike a multichannel plate/phosphor screen detector; the phosphor is imaged by a CCD camera. This image is of an unstable antiproton cloud that was initially captured off-axis in the Penning trap. The hollow profile results from diocotron oscillations of the plasma. Tracks from annihilation products can be seen in the plane of the detector

6.5 Trapping Antihydrogen for Spectroscopy: ALPHA

The ALPHA device was purpose-built to trap antihydrogen atoms so that their properties can be studied. The basic idea is to produce antihydrogen atoms at the field minimum of a magnetic gradient trap. The $\mu \cdot B$ interaction of the atoms magnetic dipole moment with the external field creates a potential well; if the atom is born with a small enough energy, it cannot escape the well and is trapped. Unfortunately, the interaction is very weak compared to what can be obtained with charged particles. For ground state antihydrogen, one obtains about 0.7 K of confinement depth for every 1 T of field change. The ALPHA trap has a well depth of about 0.5 K [31]. Thus atoms must be created with energies corresponding to less than 0.5 K in order to be trapped. When one compares this to the typical energy scales of the charged particle plasmas used to produce the neutral anti-atoms, it is clear that the task is rather daunting. The antiprotons—whose momentum determines the antihydrogen atoms momentum at production—must have meV energies when they produce anti-atoms. Recall that they start by being trapped at keV energies, and that even very careful removal of electrons leaves them at order of 100 K—to be compared to the 0.5 K trapping depth. Again, one can rely on interactions with a cyclotron-radiation cooled positron plasma to cool the antiprotons. However, in practice, the positrons don't often reach equilibrium with the cryogenic walls of the trap. The reasons for this aren't yet understood in any quantitative way, but black body radiation from warm areas of the apparatus plays a role, as does electrical noise on the Penning trap electrodes. In ALPHA we generally find that plasmas with fewer numbers of positrons equilibrate at lower temperatures; the plasmas used in the first demonstration of

trapping were typically 70–80 K, at equilibrium, and then evaporatively cooled (see discussion below) to about 40 K before mixing. These temperatures can be compared to the trap electrodes, which were at about 10 K.

The bottom line is that the charged particle temperatures achieved in the experiment to date are still quite high compared to the neutral trapping well depth. Thus one can only hope to catch a fraction of the antihydrogen atoms produced.

6.5.1 ALPHA Configuration

A schematic of the ALPHA central trapping region is shown in Fig. 6.4. The Penning trap electrodes are immediately inside the inner wall of the cryostat for the superconducting magnets that make up the neutral atom trap. An external solenoid (not pictured) provides a 1 T uniform field for the Penning trap. The atom trap magnets comprise an octupole and two solenoidal mirror coils. The resulting field has a minimum at the center of the Penning trap, where the antihydrogen is produced. The ALPHA device employs a transverse octupole—not the quadrupole generally used in Ioffe-Pritchard traps for atoms of matter. The motivation here is to try to minimize perturbations from transverse magnetic fields on the charged plasmas that are needed to form antihydrogen. Recall that most Penning traps use a very uniform axial field in order to maintain rotational symmetry. The transverse fields of the atom

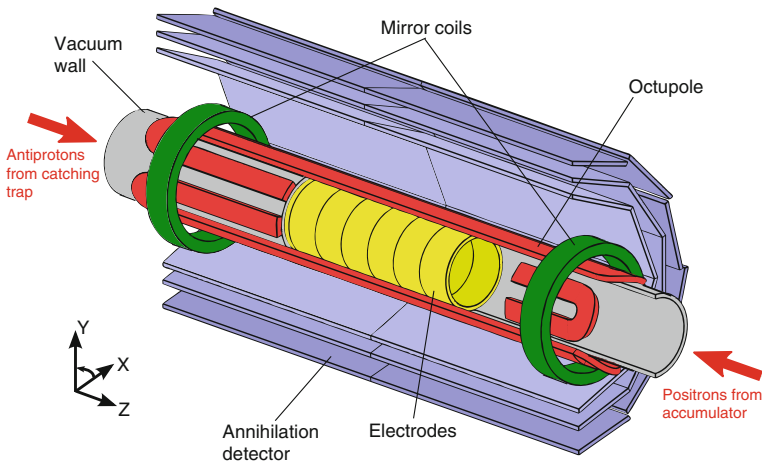


Fig. 6.4 Schematic representation of the ALPHA antihydrogen production and trapping region. The Penning trap electrodes (yellow) have an inner diameter of 44.5 mm. The inner cryostat wall and vacuum chamber wall is shown in grey. The atom trap coils are shown in green (axial confinement) and red (transverse confinement). The effective length of the atom trap is 274 mm. The modular annihilation detector is shown in a *cutaway view*; it covers the full azimuthal region. An external solenoid (not pictured) provides a 1 T axial field for the Penning trap (Reproduced from [9])

trap strongly break this symmetry. In the design stages of ALPHA, we were very concerned that these transverse fields could have a serious negative effect on stability of the positron and antiproton clouds, and experiments at Berkeley demonstrated that strong quadrupole fields had serious effects on the stability of stored electron plasmas [32]. The particles can be directly lost if their axial excursions are so long that they follow the transverse field lines into the trap wall—so called ballistic loss. This was a big concern for antihydrogen production—as the plasmas typically have to be moved together over distances that would cause such loss [32].

Fajans and Schmidt had earlier pointed out that, by using a higher-order multipole magnet, it should be possible to achieve the same total atom trap well depth while having a much flatter field profile at the axis of the Penning trap [33]. This is illustrated in Fig. 6.5 for the octupole versus quadrupole case. (An octupole—as opposed to a higher order multipole—was chosen due to practical tradeoffs in the engineering and construction of the magnets.) The operational goal then is to confine the charged particle clouds to small radii where the transverse fields are small. One of the first important results of ALPHA was to demonstrate that, in the presence of the atom trap fields, both antiprotons and positrons could indeed be trapped for times long enough to allow for antihydrogen synthesis [34]. ATRAP demonstrated antihydrogen production in a quadrupole atom trap in 2008 [35].

The ALPHA atom trap magnets are of a special construction developed by Brookhaven National Laboratory (BNL) [31]. The superconductor is wound directly onto the cryostat wall and secured with a tensioned fiberglass composite. There are no metal collars to counter the magnetic forces. This is very important for ALPHA, as the material in the magnet structure scatters the charged pions that are used to determine the antihydrogen annihilation position—the vertex. Denser material in the magnet structure leads to degraded vertex position resolution. Position sensitive

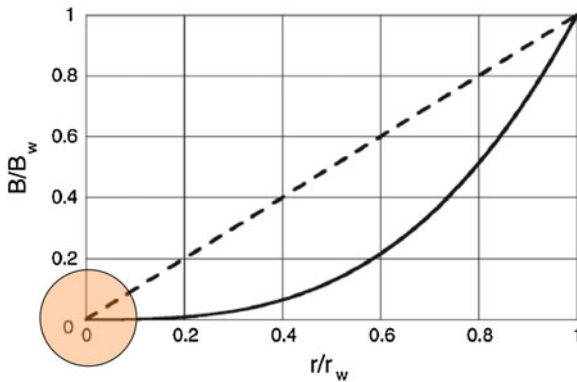


Fig. 6.5 Plot illustrating the magnetic field strength profiles for an octupole (*solid curve*) and a quadrupole (*dashed curve*). The scalar field magnitudes are normalized to the maximum field B_w at the inner wall radius r_w of the Penning trap. The maximum obtainable field is assumed to be the same for both magnet types. The *shaded region* roughly indicates the maximum radius at which plasmas are typically stored in ALPHA

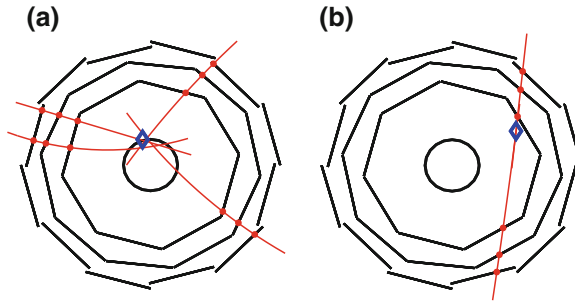


Fig. 6.6 Schematic representation (in axial projection) of event topologies in the ALPHA detector. **a** an antiproton from an antihydrogen atom annihilates on the inner wall of the Penning trap electrodes and yields four charged pions. The pion tracks (*red curves*) are reconstructed from the hit positions (*red dots*) in the three-layer silicon detector. Analysis of the tracks determines the vertex position (*blue diamond*). **b** a typical track from a cosmic ray arriving from overhead (Reproduced from [9])

detection of the antiproton annihilation has proven to be critical in all of the recent results involving trapped antihydrogen. The octupole is wound in eight distinct layers of 1 mm diameter superconductor. The effective atom trapping region is a cylindrical volume of 274 mm length and 44.5 mm diameter.

The ALPHA production and trapping region is surrounded by a three-layer, imaging vertex detector [36] comprised of segmented silicon. The detector is used to identify antiproton annihilations from lost antihydrogen, and to distinguish these from cosmic rays—which are the source of the dominant background for this experiment. The typical topologies for antiproton and cosmic ray events are shown in Fig. 6.6. Data samples of bare antiproton annihilations and cosmic ray annihilations can be collected independently of any of our antihydrogen experiments and used to develop the criteria for distinguishing signal from background in an unbiased manner. In the latest published results, we were able to reject cosmic rays to a background level of $1.7 \times 10^{-3} \text{ s}^{-1}$ [11]. Note that, unlike ATHENA, ALPHA does not have a detector for identifying the gamma rays from the positron annihilation. Absorption by the material in the cryostat and atom trap magnets precludes efficient detection of these photons. Thus we rely mainly on the antiproton annihilation detector to analyse what is happening in our experiments.

6.5.2 Detecting Trapped Antihydrogen

When the ALPHA machine was being designed in 2004–2005, it seemed unlikely that conventional ways of detecting trapped atoms of matter (e.g., by laser fluorescence) could be utilised—due to the small number of atoms expected to be trapped and the restricted geometry of the experiment itself. We thus settled on an alternative:

detection of trapped anti-atoms by controlled release from the trap and observation of the resulting annihilation. A key to this technique is rapid shutdown of the superconducting magnets in the atom trap—in order to minimise the probability that a cosmic ray arrives during the release interval. The ALPHA magnets can be de-energised with a time constant of about 9 ms. Note that this is extreme for a superconducting magnet and the experiment was not undertaken without some risk. The magnets are shut down by diverting their current (about 900 A for the octupole and 700 A for the mirror coils) to a resistor network by means of an IGBT (isolated-gate bipolar transistor) switch. The magnets quench during this shutdown, but the BNL produced magnets have survived many thousands of cycles of this treatment.

6.5.3 Antihydrogen Trapping

Ignoring many of the subtle details for now, the sequence for trapping antihydrogen involves preparing plasmas of antiprotons and positrons in adjacent wells, with the positrons centered in the atom trap. The atom trap magnets are then energized, and the plasmas are mixed to form antihydrogen. After the mixing the Penning potentials are removed and pulsed electric fields are used to remove any un-reacted charged particles that may be mirror-trapped by the atom trap magnetic fields [37].

Then the magnets are shut down, and we analyze the annihilation detector output for events resulting from antihydrogen annihilation during the release interval (typically 30 ms). To be certain that any released particles are neutral antihydrogen and not bare antiprotons, we apply an axial electric field to the trap volume while the trap is being shut down and look for evidence of displacement of the annihilation vertex positions under influence of the fields. Data sets are accumulated with fields in one axial direction left, the opposite direction right, and with no field. Figure 6.7 shows the results of the first published experiment [9]. We observed 38 events consistent with the release of trapped antihydrogen, out of 335 attempts. The expected background for the total sample was 1.4 ± 1.4 events. The antihydrogen would have been held for at least 172 ms, which is the time necessary to perform the field manipulations to remove any remaining trapped particles. The axial distribution of the annihilation positions is consistent with computer simulations of the release process for neutral antihydrogen and completely inconsistent with simulations for release of mirror trapped antiprotons [9, 37]. Refinements during the 2010 and 2011 AD running periods led to an improvement in the initial trapping rate (about one in nine attempts) to about one trapped atom per attempt [10]. An attempt takes about 20 min of real time.

6.5.4 Holding Antihydrogen

An obvious next question is How long can one hold onto trapped antihydrogen? We investigated this by simply delaying the shutdown of the magnets in our usual

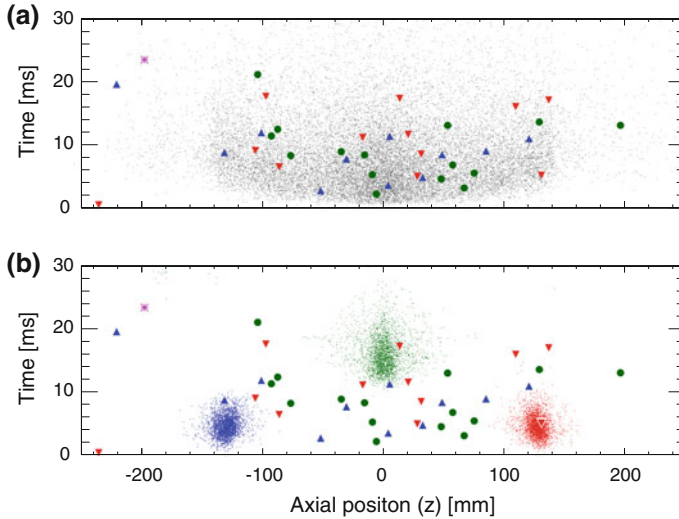


Fig. 6.7 Data and simulation of annihilation events from particles released from the ALPHA antihydrogen trap. The axial position of an annihilation is plotted versus the time from the initiation of the shutdown of the trap magnets. The measured data are the *green circles* (no axial deflection field), *red triangles* (axial field to deflect antiprotons to the right), and *blue triangles* (axial field to deflect antiprotons to the left). The measured data set is compared to **(a)** computer simulations of the release of trapped antihydrogen (*grey dots*) and **(b)** computer simulations of the release of mirror trapped antiprotons (coloured dots corresponding to the bias fields described above). One background point (*purple star*) was obtained with conditions (*heated positrons*) under which no trappable antihydrogen should have been produced (Reproduced from [9])

trapping sequence to study the survival rate at various times. The short answer is that there is clear evidence for trapped antihydrogen after 1,000 s of hold time [10], Fig. 6.8. About half of the atoms survive for this time. We have yet to investigate any loss mechanisms in detail (there may be multiple mechanisms with different time scales) or to carefully study longer times—these measurements are quite frankly rather tedious. But 1,000 s is a very long time on an atomic scale and is sufficient to allow one to contemplate spectroscopic measurements and laser cooling—even for just one atom trapped at time. The long hold times also guarantee that the trapped antihydrogen—which may have been initially trapped in a positronic excited state—has decayed to the ground state [10]. This is an extremely important point, as ground state antihydrogen is the object we wish to study precisely—for example using the 1s–2s transition. This transition in material hydrogen has been measured very precisely (a fractional frequency uncertainty of 4.2×10^{-15}) and referenced to a frequency standard by the Hänsch group [38]. Comparison of the frequencies of this transition for hydrogen and antihydrogen is one of the longest-standing goals of the AD physics program.

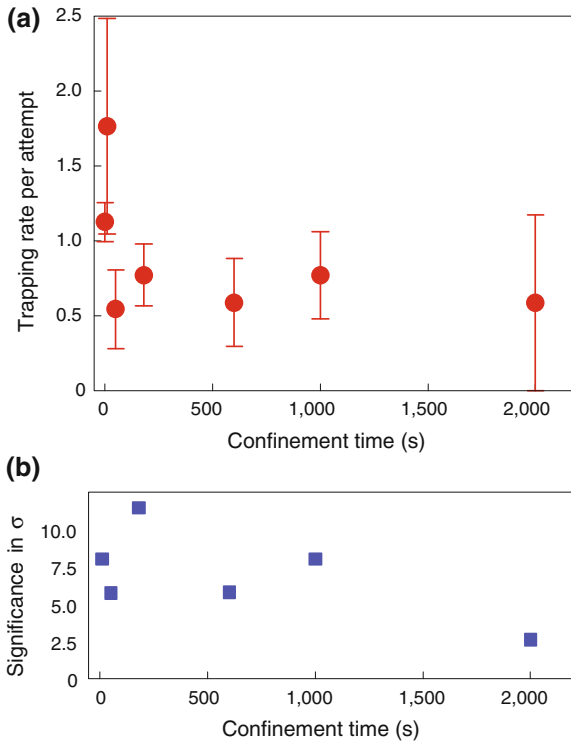


Fig. 6.8 Determination of the storage lifetime of trapped antihydrogen in the ALPHA trap. **a** The average number of antihydrogen atoms released per attempt is plotted versus the holding time. The error bars are due to counting statistics. **b** statistical significance of the data points in the graph above, expressed in σ (Reproduced from [10])

6.5.5 Measuring Trapped Antihydrogen

The original ALPHA device was not equipped with windows to allow laser access to the trapping volume, but we were able, in the shutdown between the 2010 and 2011 AD runs, to modify the apparatus to allow for axial injection of microwaves into the anti-atom trapping volume. The goal of this modification was to try to observe resonant quantum transitions between the ground-state hyperfine levels in trapped antihydrogen. The microwaves were introduced using a vacuum mounted horn antenna that could be manipulated onto the experiments access. Of the four ground state hyperfine levels, two are low-field seeking (the energy level increases with B -field) and can be trapped in the minimum- B trap. The other two states are high field seeking and untrappable. The idea behind this experiment was to resonantly drive microwave transitions between these two level manifolds [11]. The anti-atoms that make a transition go from being trapped to being untrappable and are thus lost. The transition corresponds to a positron spin flip. The experiment is conducted in

the same way as the storage time experiment. Atoms are trapped and held, and while being held they are illuminated with microwaves for some time (180 s in this case). After the irradiation, the trap is released to see if any atoms remain trapped.

Three types of data sets are accumulated: microwaves on resonance, microwaves off resonance, and no microwaves present. In this case on resonance” means resonant with the minimum field in the highly inhomogeneous trap—obviously the field varies greatly over the trapping volume. (Note that both of the low field seeking states were addressed by alternating the microwave frequency back and forth between the two during the irradiation interval.) It turns out that we could clearly see the effects of the microwaves in the release data: the resonant microwaves effectively empty the trap; using no microwaves or off-resonant microwaves does not [11]. We were also able to directly detect the annihilation of the atoms when their spin-flip occurred. This was a rather simple on-off measurement—the off-resonant microwaves were detuned 100 MHz from the roughly 29 GHz resonant field, and we did not attempt to scan the frequency to measure a line shape. Nevertheless, it represents the first-ever resonant interaction with an anti-matter atom, and demonstrates that it is possible to do some interesting physics with just a few anti-atoms (the total sample here was about 100 atoms detected).

6.5.6 Trapped Antihydrogen and Ion Trap Physics

As mentioned above, producing antihydrogen in the first place requires the successful and reliable implementation of many manipulation and diagnostic tools for Penning traps. In addition to the ones summarized above, a few innovations that are unique to ALPHA are worth mentioning, as they are directly related to producing cold antihydrogen. We attempted for many years to trap antihydrogen using ATHENA-type mixing. These attempts failed to produce any antihydrogen cold enough to be trapped—at least at the level of our sensitivity and patience. Two techniques have been particularly important to our success: autoresonant injection of antiprotons into a positron plasma and evaporative cooling of charged particle plasmas. These are described briefly below; again the details can be found in the references.

6.6 Autoresonant Injection of Antiprotons into a Positron Plasma

As described above, in ATHENA the antiprotons were injected into the positron plasma with relative energies of many electron volts. There was evidence, both from ATHENA [20] and ATRAP [39], that this type of mixing produced hot antihydrogen of perhaps hundreds of degrees K. Simulations suggested that the antihydrogen forms before the antiprotons cool into thermal equilibrium in the positron plasma [40].

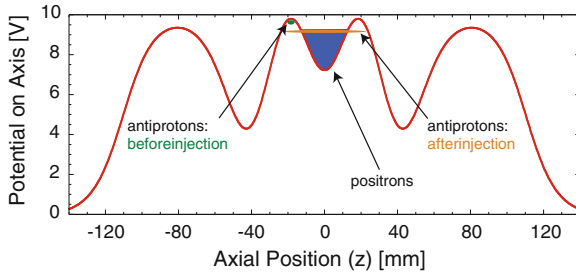


Fig. 6.9 Representation of the axial potential used for autoresonant injection of antiprotons in ALPHA. The externally applied potential is shown in *red*. The positron space charge significantly flattens the total potential in the center of the nested well

As mentioned above, the inability of ALPHA to trap antihydrogen atoms produced at the ATHENA tends to confirm this expectation. The scheme for autoresonant (see [41]) injection can be illustrated with help of Fig. 6.9. The positron and antiproton plasmas are prepared in adjacent wells. Both plasmas can be cooled in-situ by evaporative cooling—see discussion below. The axial motion of the antiprotons in the potential well is driven by applying a periodic signal to one of the Penning electrodes. Under the correct conditions of drive strength and plasma density and temperature, the antiproton cloud will behave as a coherent macroparticle [42]. The nested well shape for the antiprotons results in nonlinear behaviour: the frequency at the bottom of the antiproton well (the antiproton starting position in Fig. 6.9) is higher than that at the energy level at which the antiprotons would enter the positron plasma. The cold antiproton cloud is captured by the drive in the linear part of the well and the frequency is then swept from high to low. The antiproton cloud autoresonantly follows the drive (downward in Fig. 6.9)—matching its axial oscillation amplitude to the corresponding frequency determined by the well shape. By careful control of this frequency sweep, the antiprotons can be injected into the positron plasma with very small relative velocity—allowing for production of cold antihydrogen. All of the antihydrogen trapped in ALPHA has been produced with this kind of mixing, but this technique is still relatively new and has yet to be fully exploited. A theoretical study involving simulations of the plasma behaviour under autoresonant injection was recently published [43] and gives some guidance for optimising this technique in the future.

6.7 Evaporative Cooling of Charged Antimatter Plasmas

The technique of evaporative cooling is a mainstay of cold atom research [44]. In ALPHA, we have applied this technique to both antiprotons [45] and positrons in our efforts to create trappable antihydrogen (see [46] for a description of the experimental situation before evaporative cooling was introduced).

As noted above, the positron plasmas in our machine do not reach thermal equilibrium with the cryogenic trap walls (10 K). The antiproton plasmas are usually left at a temperature of a few hundred K after electron removal. In order to improve this situation we can evaporatively cool both species by simply reducing the Penning trap well depth to allow warmer particles to escape. We have earlier cooled a sample of antiprotons to about 9 K using this technique [45]. This of course involves throwing away precious antimatter particles, but the idea is to end up with more particles that can produce trappable antihydrogen.

For positrons, the situation is not very dire; we can easily trap close to 10^8 positrons, but we use only about 2 million positrons in the successful antihydrogen trapping experiments. It hurts more to throw away antiprotons—we only have about 40,000 to start with, but current thinking suggests that the positron temperature still plays the dominant role, as the antiprotons quickly equilibrate when they are gently introduced by the autoresonant technique.

Indeed, our first hint of antihydrogen trapping came in 2009, when we saw six candidate events in 212 attempts with positrons at about 70 K [46]. These measurements were taken without the electrical bias fields that ensure that the events were not due to mirror-trapped antiprotons, but simulations indicate that it is very unlikely that these were charged events. The most substantial change between the 2009 and 2010 runs was the introduction of evaporative cooling to the positron plasma. This resulted in positrons of about 40 K, and the measured trapping rate of one atom in about nine attempts.

While the antiproton temperature may only have a higher order effect on the efficiency of the current mixing technique, evaporative cooling can in principle lead to better control and reproducibility of the autoresonance injection. In other mixing techniques in which the antiproton plasma is stationary—for example, interaction of an antiproton cloud with positronium atoms [47], evaporative cooling could be a very important tool for increasing the number of trapped atoms. Both ATRAP and AEGIS use variations of the positronium technique. Efforts in ALPHA will continue to reduce the positron plasma temperature, as well as optimization of the whole production cycle to increase the number of trapped atoms per attempt. Madsen [48] is pursuing the use of sympathetic cooling of positrons by laser cooled trapped ions, as demonstrated by the Bollinger group [49], to reduce the positron temperature. This project is funded and just beginning to be implemented for ALPHA.

6.8 Towards Antihydrogen Spectroscopy

At the time of the writing of this chapter (Summer 2013), the AD is currently shut down in connection with the upgrade of the LHC machine, and we will not see antiproton beam again before mid-2014 at the earliest. To prepare for the next generation of experiments with antihydrogen, we have (in 2012) constructed a completely new experimental apparatus, known as ALPHA-2. A schematic diagram is shown in Fig. 6.10. As mentioned above, the original ALPHA machine did not allow for

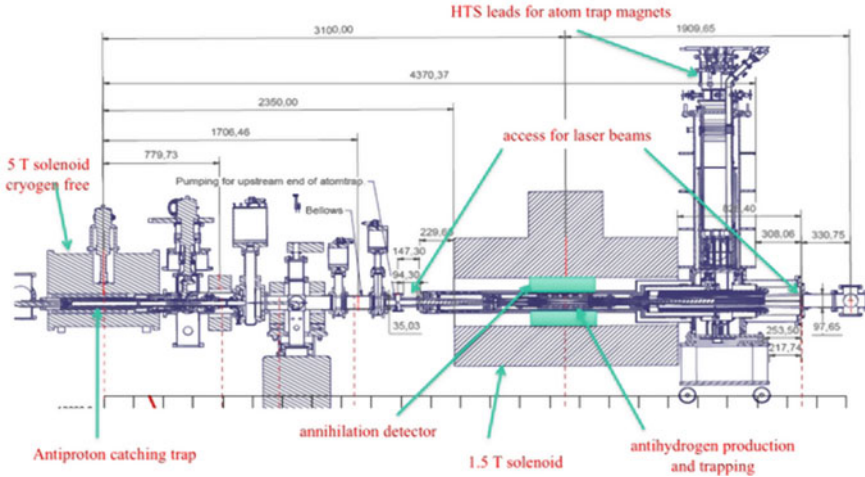


Fig. 6.10 Graphic depiction of the ALPHA-2 device. The antiprotons from the AD (arriving from the left of the figure) are caught, cooled and accumulated in a separate trap with its own solenoid magnet. The atom trap features a similar construction to that of the original ALPHA machine, but with added solenoidal coils for tailoring the longitudinal field shape. Current is introduced to the magnets (eight individual coils) through high temperature superconducting leads developed for the LHC

access of laser beams to the anti-atom trapping volume. ALPHA-2 remedies this by including access and egress windows for up to four laser beams. One of the laser paths features a Fabry-Perot buildup cavity within the cryogenic UHV system to allow for power enhancement of the 243 nm laser light needed for the two-photon excitation of the $1s-2s$ transition. Investigation of this transition has been one of the goals of the collaboration since its inception. We hope to begin initial investigations of this line with ALPHA-2 when the AD beam returns.

Some ALPHA colleagues have recently considered the feasibility of laser cooling of trapped antihydrogen atoms using pulsed Lyman- α light [50]. The potential for this is also included in the design of ALPHA-2, and the necessary laser is being developed within the collaboration. We will also continue our microwave investigations. ALPHA-2 features extra magnetic coils that will allow us to flatten the longitudinal field profile in the trap center, yielding a larger resonant volume for the microwave transitions. We eventually hope to probe the antihydrogen NMR (nuclear magnetic resonance or antiproton spin flip) transitions using trapped antihydrogen, but some technical development remains to allow injection of the required wavelength into the trapping volume. Meanwhile, ASACUSA is actively pursuing their Ramsey-type drift experiment [14] to measure the hyperfine spectrum. I will refrain from making predictions about how the development of antihydrogen spectroscopy will proceed—these always ultimately lead to embarrassment. It is in many ways remarkable that we are now in a position to design real measurements using trapped antimatter atoms—the landscape was somewhat bleaker a few short years ago. Clearly we would like

to have more trapped atoms per attempt, and the truly precision experiments may require vastly different experimental setups than those we have now. I remain confident that this inexhaustible and creative community of physicists will overcome the necessary obstacles to answer the very fundamental and intriguing question: Do atoms of matter and antimatter obey the same laws of physics?

To aid us in this quest, CERN has recently approved a major upgrade to the AD complex. The ELENA ring will further decelerate antiprotons from the AD down to 100 keV. This will allow researches to capture a much higher fraction of the delivered antiprotons and allow us to make more rapid progress in our research. The entire community is looking at a very bright future for low energy antiproton physics.

6.8.1 Dropping Antihydrogen

Although this is a volume about spectroscopy, we note in passing that ALPHA has recently published the first experimental study to directly address gravitational effects on neutral antimatter [12]. The concept is simple—we looked at the position distribution of the annihilation vertices due to antihydrogen atoms that were intentionally released from the trap. This was not an experiment per se, but a retrospective analysis of data taken in the course of other experiments. The antihydrogen in ALPHA is typically too warm (recall the well depth is up to about 0.5 K) that we would expect to see the effect of gravitational free fall when the atoms are released in the horizontally oriented atom trap. However, there is a distribution of energies, and the coldest atoms can be expected to emerge later in the release process, as the confining potential decays. So while we cannot directly observe free fall (or upward acceleration, for antigravity), we can compare the measurements to computer simulations of the release of trapped atoms. In the simulations, we can assume that the gravitational mass of antihydrogen is different from its inertial mass by some ratio F . By statistically comparing the data with simulations of varying F , we can use the data to place limits on F . The answer is that F lies between -65 and 110 (negative signs imply antigravity). This is not a very interesting band yet, but the experiment shows how one might approach such measurements with trapped antihydrogen, and we have examined the improvements that could be made to this technique in the future. It is not unreasonable to expect to be able to rule out $F = -1$ (antigravity) with this technique in the not too distant future. Both AEGIS and Gbar will aim for more precise measurements of the value of g for antiatoms. These are both very technically challenging experiments.

Acknowledgments The author would like to thank the editors, Professors Quint and Vogel, for taking the initiative to prepare this volume and for the hard work of editing it. My many colleagues in PS200, ATHENA, and ALPHA are gratefully acknowledged for outstanding collaboration over the years; their names are to be found in the references. I would also like to thank the CERN AD and injector staff for delivering reliable beam over the years, and the members of the other AD and LEAR experiments, past and present, for creating an extremely stimulating working environment at CERN. The authors work has been supported by the Danish National Research Council (SNF, FNU), the Carlsberg Foundation, and the European Research Council.

References

1. S. Maury, The antiproton decelerator: AD. *Hyp. Int.* **109**, 4352 (1997)
2. G. Baur et al., Production of antihydrogen, *Phys. Lett. B* **368**(3), 251 (1996). Bibcode:1996PhLB.368.251B. doi:10.1016/0370-2693(96)00005-6
3. G. Blanford et al., Observation of antihydrogen, *Phys. Rev. Lett.* **80**(14), 3037 (1998). Bibcode:1998PhRvL.80.3037B. doi:10.1103/PhysRevLett.80.3037
4. G. Gabrielse et al., First capture of antiprotons in a penning trap: a kiloelectronvolt source. *Phys. Rev. Lett.* **57**, 2504–2507 (1986)
5. G. Gabrielse et al., Cooling and slowing of trapped antiprotons below 100 meV. *Phys. Rev. Lett.* **63**, 13601363 (1989)
6. C.M. Surko, R.G. Greaves, Emerging science and technology of antimatter plasmas and trapped beams. *Phys. Plasmas* **11**, 2333–2348 (2004)
7. L.V. Jorgensen et al., New source of dense cryogenic positron plasmas. *Phys. Rev. Lett.* **95**, 025002 (2005)
8. M. Amoretti et al., Production and detection of cold antihydrogen atoms. *Nature* **419**, 456459 (2002)
9. G.B. Andresen et al., Trapped antihydrogen. *Nature* **468**, 673–676 (2010)
10. C. Amole et al., ALPHA collaboration, confinement of antihydrogen for 1000 seconds. *Nat. Phys.* **7**, 558 (2011)
11. C. Amole et al., Resonant quantum transitions in trapped antihydrogen atoms. *Nature* **483**, 439 (2012)
12. C. Amole et al., Description and first application of a new technique to measure the gravitational mass of antihydrogen. *Nat. Commun.* **4**, 1785 (2012)
13. G. Gabrielse et al., Trapped antihydrogen in its ground state. *Phys. Rev. Lett.* **108**, 113002 (2012)
14. E. Widmann et al., Measurement of the hyperfine structure of antihydrogen in a beam, *Hyp. Int.* **215**, 1 (2013) (<http://dx.doi.org/10.1007/s10751-013-0809-6>)
15. Y. Enomoto et al., Synthesis of cold antihydrogen in a cusp trap, *Phys. Rev. Lett.* **105**, 243401 (2010) (<http://link.aps.org/doi/10.1103/PhysRevLett.105.243401>)
16. A. Kellerbauer et al., (AEGIS collaboration), proposed antimatter gravity measurement with an antihydrogen beam. *Nucl. Inst. Meth. B* **266**, 351 (2008). doi:10.1016/j.nimb.2007.12.010
17. P. Perez, Y. Sacquin, The GBAR experiment: gravitational behaviour of antihydrogen at rest. *Class. Quantum Grav.* **29**, 184008 (2012)
18. G. Gabrielse, S.L. Rolston, L. Haarsma, W. Kells, Antihydrogen production using trapped plasmas. *Phys. Lett. A* **129**, 38 (1988)
19. M. Amoretti et al., High rate production of antihydrogen. *Phys. Lett. B* **578**, 23–32 (2004)
20. N. Madsen et al., Spatial distribution of cold antihydrogen formation. *Phys. Rev. Lett.* **94**, 033403 (2005)
21. G. Gabrielse et al., Background-free observation of cold antihydrogen with field ionization analysis of its states. *Phys. Rev. Lett.* **89**, 213401 (2002)
22. X.-P. Huang, F. Anderegg, E.M. Hollmann, C.F. Driscoll, T.M. O'Neil, Steady-state confinement of non-neutral plasmas by rotating electric fields, *Phys. Rev. Lett.* **78**, 875 (1997)
23. G.B. Andresen et al., Compression of antiproton clouds for antihydrogen trapping. *Phys. Rev. Lett.* **100**, 203401 (2008)
24. G.B. Andresen et al., Antiproton, positron, and electron imaging with a microchannel plate/phosphor detector. *Rev. Sci. Inst.* **80**, 123701 (2009)
25. N. Kuroda et al., Radial compression of an antiproton cloud for production of intense antiproton beams. *Phys. Rev. Lett.* **100**, 203402 (2008)
26. M.D. Tinkle et al., Low-order modes as diagnostics of spheroidal non-neutral plasmas. *Phys. Rev. Lett.* **72**, 352 (1994)
27. M.D. Tinkle, R.G. Greave, C.M. Surko, Low-order longitudinal modes of single-component plasmas. *Phys. Plasmas* **2**, 2880 (1995)

28. M. Amoretti et al., Complete nondestructive diagnostic of nonneutral plasmas based on the detection of electrostatic modes. *Phys. Plasmas* **10**, 3056 (2003)
29. M. Amoretti et al., Positron plasma diagnostic and temperature control for antihydrogen production. *Phys. Rev. Lett.* **91**, 055001 (2003)
30. C. Amole et al., In-situ electromagnetic field diagnostics with an electron plasma in a Penning-Malmberg trap. *New J. Phys.* (Submitted) (2013)
31. W. Bertsche et al., A magnetic trap for antihydrogen confinement. *Nucl. Inst. Meth. A* **566**, 746 (2006)
32. J. Fajans, W. Bertsche, K. Burke, S.F. Chapman, D.P van der Werf. *Phys. Rev. Lett.* **95**, 15501 (2005)
33. J. Fajans, A. Schmidt, Malmberg-penning and minimum-B trap compatibility: the advantages of higher-order multipole traps. *Nucl. Inst. Meth. A* **521**, 318 (2004)
34. G. Andresen et al., Antimatter plasmas in a multipole trap for antihydrogen. *Phys. Rev. Lett.* **98**, 023402 (2007)
35. G. Gabrielse et al., Antihydrogen production within a penning-ioffe trap. *Phys. Rev. Lett.* **100**, 113001 (2008)
36. G. Andresen et al., The ALPHA detector: module production and assembly. *JINST* **7**, C01051 (2012). doi:[10.1088/1748-0221/7/01/C01051](https://doi.org/10.1088/1748-0221/7/01/C01051)
37. C. Amole et al., Discriminating between antihydrogen and mirror-trapped antiprotons in a minimum-B trap. *New J. Phys.* **14**, 105010 (2012)
38. C.G. Parthey et al., Improved measurement of the hydrogen 1S_{2S} transition frequency. *Phys. Rev. Lett.* **107**, 203001 (2011)
39. G. Gabrielse et al., First measurement of the velocity of slow antihydrogen atoms. *Phys. Rev. Lett.* **93**, (2004)
40. F. Robicheaux, Simulations of antihydrogen formation. *Phys. Rev. A* **70**, 022510 (2004)
41. J. Fajans, L. Friedland, Autoresonant (nonstationary) excitation of pendulums, platinos, plasmas, and other nonlinear oscillators. *Am. J. Phys.* **69**, 1096 (2001)
42. I. Barth, L. Friedland, E. Sarid, A.G. Shagalov, Autoresonant transition in the presence of noise and self-fields. *Phys. Rev. Lett.* **103**, 155001 (2009)
43. C. Amole et al., Experimental and computational study of the injection of antiprotons into a positron plasma for antihydrogen production. *Phys. Plasmas* **20**, 043510 (2013). doi:[10.1063/1.4801067](https://doi.org/10.1063/1.4801067)
44. H.F. Hess, Evaporative cooling of magnetically trapped and compressed spin-polarized hydrogen. *Phys. Rev. B* **34**, 3476 (1986)
45. G. Andresen et al., Evaporative cooling of antiprotons to cryogenic temperatures. *Phys. Rev. Lett.* **105**, 013003 (2010)
46. G. Andresen et al., Search for trapped antihydrogen. *Phys. Lett. B* **695**, 95 (2011)
47. B.I. Deutch et al., Antihydrogen by positronium-antiproton collisions. *Hyp. Int.* **44**(1–4), 271–286 (1989)
48. N. Madsen, Private Commun. (2011)
49. B.M. Jelenkovic et al., Sympathetically laser-cooled positrons. *Nucl. Inst. Meth. B* **192**, 117127 (2002)
50. P.H. Donnan et al., A proposal for laser cooling antihydrogen atoms. *J. Phys. B* **46**, 025302 (2013). doi:[10.1088/0953-4075/46/2/025302](https://doi.org/10.1088/0953-4075/46/2/025302)